Synthesis of fluorinated *anti*-fluorenacenedione and the structural, electronic, and field-effect properties†

Yasuo Miyata, Takeo Minari, Takashi Nemoto, Seiji Isoda and Koichi Komatsu*

Received 2nd May 2007, Accepted 13th June 2007
First published as an Advance Article on the web 4th July 2007
DOI: 10.1039/b706621j

Fluorinated *anti*-fluorenacenedione **6** was newly synthesized by oxidation of a dehydro[12]annulene fused with tetrafluorobenzene **4**. X-Ray crystallography of **6** demonstrated a totally planar structure and shorter intramolecular distances for F ··· I, F ··· O, and I ··· O than the corresponding sums of van der Waals (vdW) radii. In the packing structure, molecules are arranged in a π-stacked motif, and the intermolecular distances between heavy atoms (C ··· I, C ··· F, C ··· O, F ··· I, and F ··· O) of the adjacent columns are also shorter than the corresponding sums of vdW radii, indicating highly dense packing for the crystal structure of **6**. In the ^{19}F NMR spectrum of **6**, a signal for the fluorine atom adjacent to iodine exhibited downfield shift by 29–40 ppm as compared with the other three signals. This is attributed to the intramolecular short contact between F and I atoms, which is supposed to cause a donor–acceptor interaction. Cyclic voltammetry of **6** exhibited two reversible reduction waves at $E_{1/2} = -0.91$ and -1.45 V *vs.* Fc/Fc$^+$. A thin film of **6** was prepared by vacuum deposition and was applied to a field-effect transistor (FET) device, which exhibited *n*-type transistor responses although the mobility was not very high.

Introduction

Organic field-effect transistors (OFETs) have received considerable attention during the last decade. OFETs have features of flexibility as a material and low-cost in processing as compared with amorphous silicon transistors. Making the best use of these features specific to organic materials, OFETs have potential for use in applications such as backplane electronics for large-area flat panel displays, electronic papers, and so forth. For use in these applications, the development of both *p*- and *n*-type FETs is essential for the logical circuit of "inverters". So far, high mobility and on–off ratio have been attained in *p*-type FETs, but the development of *n*-type FETs has been left behind.[1] This is attributed to the instability of *n*-type FETs in air.[1,2] Radical anions as electron-transfer carriers are readily quenched by moisture and oxygen. One way to solve this problem would be dense packing in a thin film, which would prevent water and oxygen from penetrating the film. For examples, some air-stable *n*-type FETs have been prepared by the use of perfluorophthalocyanine **1**,[3] naphthalenetetracarboxylic diimide **2**,[4] and dicyanoperylenetetracarboxylic diimide **3**.[5] In the thin film of **1**, the molecules are arranged in a π-stacking motif and in a perpendicular arrangement to the substrate. The π-conjugated core of **1** is surrounded by water-repelling fluorine substituents. These factors are considered as good reasons for the film of **1** to exhibit high FET mobility in air.[3] In addition, theoretical studies[6] and experimental observations[7] have demonstrated that maximizing the overlap of π orbitals in thin films makes the carrier transfer most effective. It is obvious that a π-stacking arrangement in a thin film is a quite important structural factor for an active layer of *n*-type OFET.

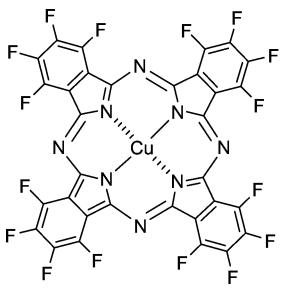

1

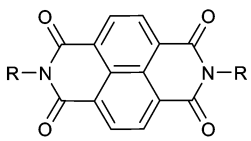

2 R = $CH_2C_7F_{15}$

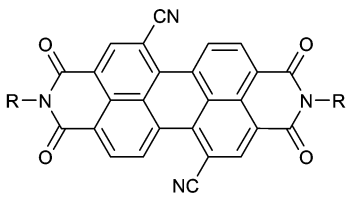

3a R = $CH_2C_3F_7$
3b R = cyclohexane

Previously, we synthesized and investigated the electronic properties and crystal structures of dehydro[12]annulene fused with tetrafluorobenzene **4**.[8] Annulene **4** was shown to have its LUMO at a considerably low energy level. In the crystal packing structure for a mixture with a nonfluorinated counterpart, an efficient π-stacked arrangement caused by a phenyl–perfluorophenyl interaction[9] was demonstrated. On the other hand, Swager and co-workers

Institute for Chemical Research, Kyoto University, Uji, Kyoto 611–0011, Japan. E-mail: komatsu@scl.kyoto-u.ac.jp; Fax: +81 774 38 3178; Tel: +81 774 38 3172

† Electronic supplementary information (ESI) available: Crystal data and structure refinement for **6**, atomic coordinates and equivalent isotropic displacement parameters for **6**, bond lengths and angles for **6**, cartesian coordinates from the optimized structure of **6** at B3LYP/6-311G(d) (3-21G* for iodine atoms), cartesian coordinates from the optimized structure of **9** at B3LYP/6-311G(d) and cartesian coordinates from the optimized structure of $CFCl_3$ at B3LYP/6-311G(d). See DOI: 10.1039/b706621j

reported that dehydro[12]annulene **5** can be oxidized with I_2 to afford *anti*-fluorenacenedione **7**.[10j] The chemistry of *anti*-fluorenacenedione derivatives, which are fully planar π-conjugated molecules having two carbonyl groups, has been studied since the 1950's.[10] Cyclic voltammetry on **8** was reported to exhibit reversible four-step four-electron reduction waves,[10g] and the radical anion and dianion of **8** were also generated by chemical reduction.[10k] However, with the exception of these reports and UV–vis absorptions of **7**,[10j] detailed properties of fluorenacenediones have not been fully examined yet.

In this paper, fluorinated *anti*-fluorenacenedione **6** was newly prepared by oxidation of **4** with I_2, and the structural and electronic properties of **6** were investigated by X-ray crystallography, UV–vis spectroscopy, electrochemistry, and theoretical calculations. The packing structure in the crystal is of particular interest since substitution by halogen atoms is expected to promote efficient π-stacking.[7b,11] In addition, since compounds having electron-withdrawing groups at both ends were reported to show *n*-type FET properties[3,12] and the π-system of **6** should be planar like pentacene, which is known to exhibit high mobility,[13] FET measurements using the vacuum-deposited thin film of **6** were carried out to elucidate its possibility for application to OFET.

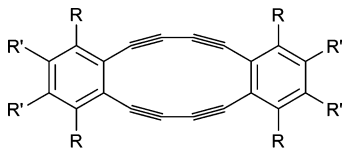

4 R = F

5 R = H R' = $C_{12}H_{25}$

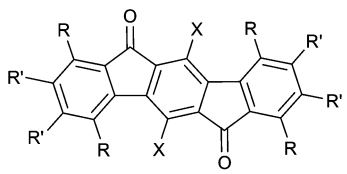

6 R = R' = F X = I

7 R = H R' = $C_{12}H_{25}$ X = I

8 R = R' = H X = H

9 R = R' = F X = H

Results and discussion

Synthesis of fluorinated *anti*-fluorenacenedione

The *anti*-fluorenacenedione with long alkyl chains (**7**) was previously synthesized in 61% yield by Swager and co-workers by oxidation of dehydro[12]annulene **5** with iodine and air for 1 h (Scheme 1).[10j] This reaction is considered to proceed through the formation of intermediate **10**, which is air-oxidized to give product **7**.[10j] Similarly, when a mixture of fluorinated dehydroannulene **4** and I_2 was stirred in benzene in air, fluorinated fluorenacenedione **6** was obtained as an orange solid in 33% yield out of a complex mixture of unknown compounds with consumption of all the starting material. The reaction was slow and took 5 days to complete. When oxygen was bubbled into the reaction mixture, the consumption of **4** was complete after 3 days, but the product yield was not improved. The lower reactivity of **4** is attributed

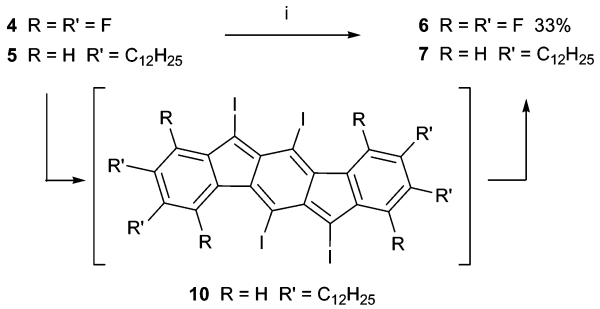

Scheme 1 *Reaction conditions:* (i) I_2, benzene, under air, 61%.

to the lower oxidizability of **4** having electron-withdrawing fluorine substituents. All attempts to remove or convert the iodo substituents to other substituents or to protect carbonyl groups were unsuccessful.

In addition to the electronic properties of π-conjugated organic compounds, their solubility, stability, and processability are also important factors for fabrication of a low-cost FET device using the solution process. Fluorenacenedione **6** is stable to light, heat, and air, although pentacene, which is known to exhibit high FET performance,[13] more readily degrades under light and air.[14] In contrast to the intractably low solubility of pentacene (<0.05 mg mL^{-1}, CH_2Cl_2), fluorenacenedione **6** is soluble in CH_2Cl_2 with a maximum concentration of 6 mg mL^{-1}.

Crystal structure of fluorinated *anti*-fluorenacenedione 6

X-Ray crystallography was conducted on a single crystal of **6** obtained by slow diffusion of hexane into a solution of **6** in CH_2Cl_2. The ORTEP drawing of the molecule exhibited a nearly planar structure as shown in Fig. 1A. The closest intramolecular distances between F and O (2.87 Å, **A** of Fig. 1A), I and O (3.08 Å, **B** of Fig. 1A), and F and I (2.97 Å, **C** of Fig. 1A) are shorter than each sum of van der Waals (vdW) radii (Table 1). Particularly, the distances between I and O and between F and I are 0.42 Å and 0.48 Å shorter than each sum of vdW radii, respectively, suggesting the presence of some electronic interaction between these atoms.[15] For example, in the HOMO-8 orbital, which was obtained by DFT calculations using the X-ray structure geometry, there appears an interaction between iodine and oxygen orbitals (Fig. 2).

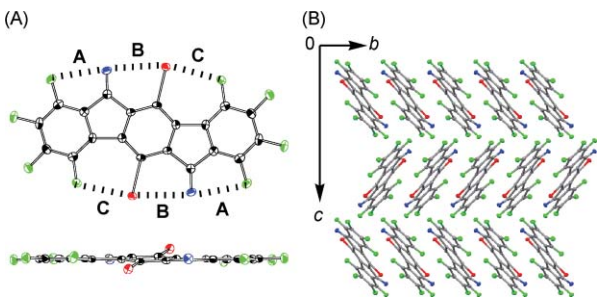

Fig. 1 (A) ORTEP drawings of the top view and side view of **6**. Thermal ellipsoids are drawn at 50% probability level. Selected distances (Å) of dotted lines **A**: F···O, 2.87; **B**: I···O, 3.08; **C**: F···I, 2.97. (B) Packing structure within the *bc* plane of **6**. Fluorine, oxygen, and iodine atoms are shown in green, blue, and red, respectively.

The packing structure of fluorenacenedione **6** is shown in Fig. 1B. The compound has π-stacked packing rather than a

Table 1 Distances (D) of intra- and intermolecular short contacts between heavy atoms of **6**, the sums of vdW radii (VDW),[a] and (D)–(VDW)

Entry	Distance (D) (Å)	Sum of vdW Radii (VDW) (Å)	(D)–(VDW) (Å)
Intramolecular distance (Fig. 1A)			
A (F···O)	2.87	2.99	−0.12
B (I···O)	3.08	3.50	−0.42
C (F···I)	2.97	3.45	−0.48
Intermolecular distance (Fig. 3)			
A (C···C) (Fig. 4)	3.31	3.40	−0.09
A (F···I)	3.37	3.45	−0.08
B (F···I)	3.25	3.45	−0.20
C (C···I)	3.67	3.68	−0.01
D (C···O)	3.04	3.22	−0.18
E (F···O)	2.98	2.99	−0.01
F (C···F)	2.98	3.17	−0.19

[a] Standard vdW radii are taken from ref. 16.

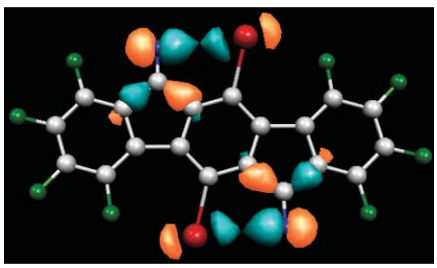

Fig. 2 The HOMO-8 orbital of **6** at a single point calculation by B3LYP/6-311+G(2d) (3-21G* for iodine atom) using the X-ray structure geometry.

herringbone arrangement. The distance between carbon atoms of facing benzene rings (C···C) along the π-stacked column axis is shown to be 3.31 Å, which is shorter than the sum of vdW radii (Fig. 3 and Table 1). The crystal structures of most of the molecules used as active layers of OFET are reported to have the herringbone arrangement as in the cases of oligothiophenes[6a,17] and pentacene,[6a] but it is also known that π-stacked packing is advantageous for more effective carrier transfer than the herringbone packing.[6,7] Besides, the intermolecular distances between heavy atoms (F···I, C···I, C···O, C···F, and F···O) of adjacent columns are shorter than the sums of vdW radii (Fig. 4 and Table 1). In particular, intermolecular distances between C and F and between C and O are remarkably short ((D)–(VDW) = −0.19

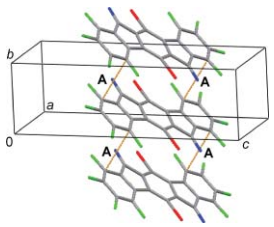

Fig. 3 Packing structure of **6** along the π-stacked column axis. Orange lines exhibit the short distances (**A**) between facing C atoms, with a distance of 3.31 Å.

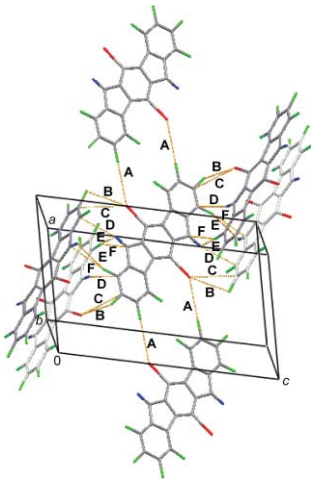

Fig. 4 Packing structure of **6** with the adjacent molecules. Orange lines exhibit the distances (Å) between heavy atoms shorter than the sums of vdW radii. **A**: F···I, 3.37; **B**: F···I, 3.25; **C**: C···I, 3.67; **D**: C···O, 3.04; **E**: F···O, 2.98; **F**: C···F, 2.98.

and −0.18 Å, respectively, Table 1). Therefore, the fluorinated fluorenacenedione could be applied as an active layer of FET since such short contacts between heavy atoms should promote highly ordered and dense packing.

^{19}F NMR of fluorenacenedione 6

The observed short intramolecular distance between F and I should be reflected in the ^{19}F NMR chemical shift. As shown in Fig. 5A, one of the four ^{19}F signals was found to be downfield shifted from the rest of the signals by 29–40 ppm. The signal assignment was made by comparison of the experimental ^{19}F NMR spectrum with that obtained by GIAO calculation. The most downfield-shifted signal was assigned to the fluorine atom that is close to the iodine atom (Fig. 5B). This signal was shown to be downfield shifted by 31–47 ppm as compared with the signals for the rest of fluorine atoms. No such downfield shift was predicted for the spectrum for **9** with iodine atoms removed (Fig. 5C), indicating that this downfield shift is attributed to an electronic interaction between F and I. Since the downfield shift is related to the decrease in electron density, this interaction is considered as the one with a donor (fluorine)–acceptor (iodine) type. It is suggested that the short contact between F and I is due to this donor–acceptor type interaction.

Electronic properties

The UV–vis spectrum of fluorinated fluorenacenedione **6** measured in CH_2Cl_2 showed the longest wavelength absorption at 479 nm with a shoulder at 505 nm (Fig. 6), while non-fluorinated fluorenacenedione **7** was reported to exhibit the longest wavelength absorption only at 316 nm.[10j] The absorption in the visible wavelength-region should be common to these two compounds since both have an orange color[10j] as solids.

In order to examine the redox behavior of **6**, cyclic voltammetry (CV) was carried out in CH_2Cl_2. As shown in Fig. 7, two reversible reduction waves were clearly observed at the potentials of $E_{1/2}$ −0.91 and −1.45 V *vs.* Fc/Fc^+. In the case of fluorenacenedione **8** having no halogen substituents, the CV in DMF has been reported

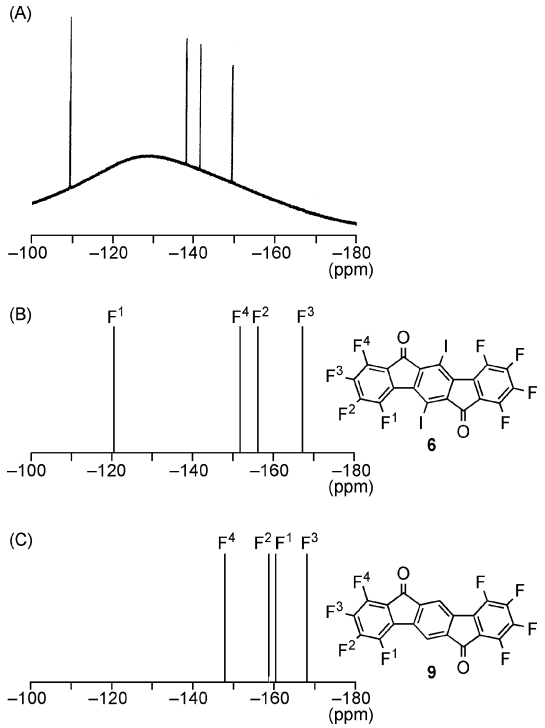

Fig. 5 (A) The experimental ^{19}F NMR spectrum of **6** with the fluorine chemical shift with reference to $CFCl_3$. ^{19}F NMR spectra (B) of **6** and (C) of **9**, calculated at GIAO-B3LYP/6-311+G(2d)//B3LYP/6-311G(d) (3-21G* for iodine atom).

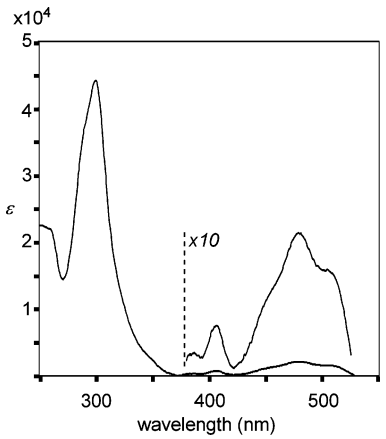

Fig. 6 UV–vis absorption spectra of **6** in CH_2Cl_2.

to exhibit four-step reversible reduction waves at $E_{1/2}$ −1.14, −1.49, −1.71, and −2.39 V *vs.* Fc/Fc^+.[10g,18] Compound **8** has been also shown to be chemically reduced to the radical anion and dianion by naphthalene radical anion.[10k] Apparently, the lower reduction potential in **6** (−0.91 V) is ascribed to the perfluoro substituents. This first reduction potential of **6** is even lower than that of perfluoropentacene (−1.13 V in 1,2-dichlorobenzene *vs.* Fc/Fc^+)[19] and C_{60} (−1.14 V in 1,2-dichlorobenzene *vs.* Fc/Fc^+),[19] which have been reported to show satisfactory performance in *n*-type FETs.[19,20] This relatively low LUMO level of fluorinated fluorenacenedione **6** would be advantageous for effective electron transfer in an active layer of *n*-type FET.

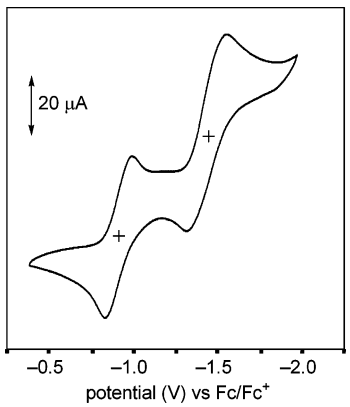

Fig. 7 Cyclic voltammogram of **6** (1.0 mM) in CH_2Cl_2 containing $Bu_4N^+ClO_4^-$ (0.1 M) with a scan rate of 100 mVs^{-1}.

OFET characteristics

Motivated by the above-mentioned properties of fluorinated fluorenacenedione **6**, we fabricated an OFET using **6** on a $Si–SiO_2$ substrate with a top-contact structure. The FET measurements of the device using a film prepared by vacuum deposition were carried out under vacuum (10^{-3} Pa) and also under air. For details of the device, see the Experimental section. Fig. 8 illustrates the drain current (I_D) *vs.* drain voltage (V_D) curves observed for **6** on the substrate at various gate voltages (V_G). The field-effect mobility (μ) was determined from the saturation region, and an on–off ratio was calculated from the I_D between $V_G = 0$ and 100 V. The FET performances of **6** under vacuum and under air are summarized in Table 2.

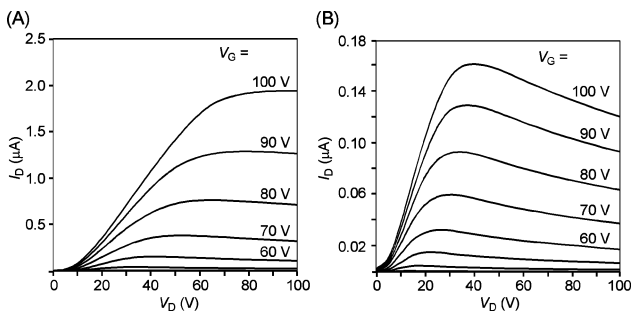

Fig. 8 Plots of drain-source current (I_D) *vs.* drain-source voltage (V_D) for an FET device fabricated with fluorenacenedione **6**, measured (A) under vacuum (10^{-3} Pa) and (B) under air.

Thus, the present OFET device using the vacuum-deposited thin film of **6** shows *n*-type transistor responses, although the observed mobilities are low both under vacuum and under air. The lower

Table 2 Field-effect mobility (μ), on–off ratio, and threshold voltage (V_T) for transistors of **6**

Condition	μ ($cm^2\ V^{-1}\ s^{-1}$) (*type*)	On–off Ratio	V_T (V)
Vacuum[a]	2.93×10^{-5} (*n*)	10^5	48
Air	6.08×10^{-6} (*n*)	10^3	35

[a] 10^{-3} Pa.

mobility and on–off ratio measured under air are probably due to the influence of oxygen and moisture, as is also indicated in the current–voltage curves shown in Fig. 8B. The observed low mobilities of the device can be explained as a result of poor film morphology of the thin film. In fact, AFM images exhibited that not grains but microcrystals were grown on an amorphous layer and the thin film deposited on the substrate was not uniform (Fig. 9). Although an appropriate reason for the observed poor morphology cannot be found at present, it is noted that Bao and co-workers also reported that vacuum-deposited films of chlorinated tetracenes exhibited a similarly poor morphology[7b] in contrast to a thin film of parent tetracene, which shows highly ordered arrangements and high FET performance.[21] It can be assumed that the film morphology and FET performance may be improved if an FET device was constructed using fluorinated fluorenacenedione, which does not carry iodine substituents. Unfortunately, however, all our attempts to remove iodine from **6** have not been successful so far.

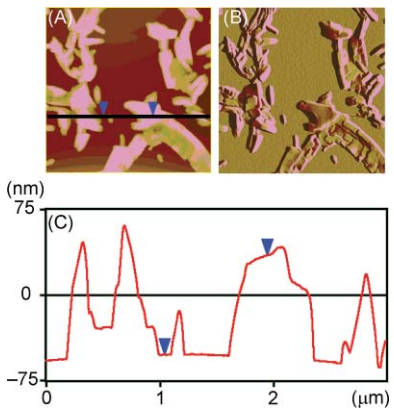

Fig. 9 (A) AFM image, (B) differential image, and (C) height profile (3 × 3 μm) of the vacuum-deposited film of **6** on a Si–SiO_2 substrate.

Conclusions

The physical, electronic, and structural properties of newly synthesized fluorinated fluorenacenedione **6** were fully elucidated. Compound **6** has an advantage of much higher solubility in common organic solvents than pentacene, which is known to exhibit high OFET performances. The crystal structure of **6** has a highly ordered arrangement, which is characterized by dense π-stacked packing. The results of X-ray crystallography and ^{19}F NMR measurements, combined with GIAO calculations, suggested the intramolecular short contact between F and I, which is ascribed to a donor–accepter interaction. The cyclic voltammogram of **6** with two stepwise reversible reductions at relatively low reduction potentials ($E_{1/2} = -0.91$ and -1.45 V *vs.* Fc/Fc^+) exhibited that **6** has a low LUMO level. A thin film of fluorinated fluorenacenedione **6** was readily prepared for use in an organic FET device. This film was found to exhibit *n*-type FET characteristics although the efficiency was low presumably due to the poor morphology. This might be improved by removal of bulky iodine atoms from **6**, and studies along this line, as well as an investigation into single-crystal FET using **6**, are now in progress.

Experimental

Measurements and materials

The melting point was determined on a Yanaco MP-500D apparatus and is uncorrected. Elemental analyses were performed at the Microanalysis Division of Institute for Chemical Research, Kyoto University. ^{19}F (372.35 MHz) and ^{13}C (99.45 MHz) NMR spectra were recorded on a JEOL JNM-AL400 spectrometer. The ^{19}F NMR chemical shifts are expressed in ppm from $CFCl_3$ as determined with reference to the external fluorobenzene (δ −113.0). The ^{13}C NMR chemical shifts are expressed in ppm from tetramethylsilane as determined with reference to CD_2Cl_2 (δ 53.8) solvent used as an internal standard. Preparative gel-permeation chromatography (GPC) was performed with a JAI LC-918 chromatograph equipped with JAIGEL 1H and 2H columns. The UV–vis spectrum was recorded on a Shimadzu UV-3150 spectrometer. The mass spectrum was obtained on a JEOL JMS700 spectrometer. AFM images of the evaporated thin film on Si–SiO_2 substrate were obtained by using a Digital Instruments Nanoscope IIIa microscope in air. Ultraviolet-ozone cleaner is a commercial product of the Nippon Laser & Electronics Lab (NL-UV253S).

All commercially available materials were of reagent grade unless otherwise noted. Dehydro[12]annulene fused with tetrafluorobenzene **4** was synthesized according to a literature procedure.[8] SiO_2 substrate was thermally grown by Miyazaki Oki Electric Co., Ltd., using a highly doped n^+-Si wafer purchased from International Test & Engineering Services Co. Ltd.

Computational method

All calculations were conducted using the Gaussian 98 program.[22] The geometry optimizations were performed with the restricted Becke hybrid (B3LYP) at 6-311G(d) (3-21G* for iodine atom) levels of theory. The GIAO calculations and the single-point calculation to estimate the Kohn–Sham LUMO level were calculated at B3LYP/6-311+G(2d) (3-21G* for iodine atom) using the geometries optimized at the B3LYP/6-311G(d) (3-21G* for iodine atom) levels.

Fluorinated *anti*-fluorenacenedione 6

Dehydro[12]annulene fused with tetrafluorobenzene **4** (486 mg, 1.24 mmol) and I_2 (189 mg, 1.49 mmol) were dissolved in benzene (350 mL) under air, and the mixture was stirred at rt for 5 days. After removal of the solvent under reduced pressure, a 10% aqueous solution of $Na_2S_2O_3$ and CH_2Cl_2 were added to the residue. Two layers were separated, and the aqueous layer was extracted with CH_2Cl_2. The combined organic solution was dried over $MgSO_4$. The solvent was removed under reduced pressure, and the crude product was purified by preparative GPC eluted with toluene to afford fluorenacenedione **6** (280 mg, 33.3%) as an orange solid. An analytically pure sample was obtained by reprecipitation from CH_2Cl_2 and hexane: mp 293.9–294.9 °C; UV–vis (CH_2Cl_2) λ_{max} 301 nm (log ε 4.64), 406 (2.88), 479 (3.33), 505 sh (3.20); ^{19}F NMR (CD_2Cl_2) δ −109.2 (ddd, J = 7.3, 14.6, 22.9 Hz), −137.9 (ddd, J = 9.6, 14.6, 20.2 Hz), −141.3 (ddd, J = 9.6, 17.4, 22.9 Hz), −149.2 (ddd, J = 7.3, 17.4, 20.2 Hz); ^{13}C NMR (CD_2Cl_2) δ 184.0, 152.9, 147.2, 145.8, 142.4, 142.0, 141.1, 122.5,

116.9, 86.1; HRMS (FAB) calcd for $C_{20}F_8I_2O_2$ 677.7850, found 677.7839. Anal. Calcd for $C_{20}F_8I_2O_2$: C, 35.43; F, 22.42; I, 37.43. Found: C, 35.34; F, 22.34; I, 37.01%.

X-Ray structural analysis of 6

Intensity data were collected at 100 K on a Bruker SMART APEX diffractometer with Mo Kα radiation ($\lambda = 0.71073$ Å) and graphite monochrometer. The structure was solved by direct methods (SHELXTL) and refined by the full-matrix least-squares on F^2 (SHELXL-97). All non-hydrogen atoms were refined anisotropically. The molecule lies about an inversion centre. $C_{20}F_8I_2O_2$; FW = 678.00, crystal size 0.20 × 0.05 × 0.05 mm^3, monoclinic, $P2_1/n$, $a = 10.9780(15)$ Å, $b = 4.7347(6)$ Å, $c = 16.960(2)$ Å, $\beta = 108.412(2)°$, $V = 836.43(19)$ Å^3, $Z = 2$, $D_c = 2.692$ g cm^{-3}. The refinement converged to $R_1 = 0.0244$, w$R_2 = 0.0600$ ($I > 2\sigma(I)$), GOF = 1.002.‡

Cyclic voltammetry

Cyclic voltammetry was performed using a standard three-electrode cell consisting of a glassy-carbon working electrode, a Pt-wire counter electrode, and a Ag/$AgNO_3$ (CH_3CN) reference electrode, under an argon atmosphere. The measurements were conducted using 1.0 mM solutions of **6** in CH_2Cl_2 with tetrabutylammonium perchlorate as a supporting electrolyte (0.1 M). The observed redox potentials were calibrated with ferrocene, as an internal standard, added after the measurement.

FET device preparation

OFETs were fabricated in a top-contact manner as follows. For devices fabricated by vacuum deposition, the gate was a highly doped n^+-Si wafer, and the gate insulator was a 600 nm thick layer of thermally grown SiO_2. After ultrasonication in acetone and then in isopropanol for 10 min each and ultraviolet-ozone-cleaner treatment for 15 min to remove organic surface contaminants, thin films of **6** (35 nm) were formed on the SiO_2 substrate held at rt by high-vacuum deposition (10^{-5} Pa). Gold source and drain electrodes (40 nm), which were thermally evaporated on the organic layer through a comb-type shadow mask, were composed of 49 pairs of comb-type electrodes with a channel length of 25 μm and a channel width of 4 × 49 mm. Characteristics of drain current (I_D) *vs.* drain voltage (V_D) of the OFET devices were measured under vacuum (10^{-3} Pa) and under air. The field-effect mobilities (μ) were calculated in the saturation region of the I_D using the equation $I_D = (WC_i/2L)\,\mu\,(V_G - V_T)$,[2] where C_i is the capacitance of the SiO_2 insulator ($C_i = 5.8 \times 10^{-8}$ F cm^{-2} (600 nm)) and V_G and V_T are the gate and threshold voltages, respectively.

Acknowledgements

We thank Dr Daisuke Yamazaki, Institute for Chemical Research, Kyoto University, for his help in X-ray structural analysis. Y. M. thanks JSPS for a Research Fellowship for Young Scientists.

‡ CCDC reference number 645703. For crystallographic data in CIF or other electronic format see DOI: 10.1039/b706621j

Notes and references

1 C. D. Dimitrakopoulos and P. R. L. Malenfant, *Adv. Mater.*, 2002, **14**, 99.
2 (*a*) D. M. de Leeuw, M. M. J. Simenon, A. R. Brown and R. E. F. Einerhand, *Synth. Met.*, 1997, **87**, 53; (*b*) F. Würthner, *Angew. Chem., Int. Ed.*, 2001, **40**, 1037; (*c*) C. R. Newman, C. D. Frisbie, D. A. da Silva Filho, J.-L. Brédas, P. C. Ewbank and K. R. Mann, *Chem. Mater.*, 2004, **16**, 4436.
3 Z. Bao, A. Lovinger and J. Brown, *J. Am. Chem. Soc.*, 1998, **120**, 207.
4 H. E. Katz, A. J. Lovinger, J. Johnson, C. Klok, T. Siegrist, W. Li, Y.-Y. Lin and A. Dodabalapur, *Nature*, 2000, **404**, 478.
5 B. A. Jones, M. J. Ahrens, M.-H. Yoon, A. Facchetti, T. J. Marks and M. R. Wasielewski, *Angew. Chem., Int. Ed.*, 2004, **43**, 6363.
6 (*a*) J. Cornil, D. Beljonne, J.-P. Calbert and J.-L. Brédas, *Adv. Mater.*, 2001, **13**, 1053; (*b*) J.-L. Brédas, J.-P. Calbert, D. A. da Silva Filho and J. Cornil, *Proc. Natl. Acad. Sci. U. S. A.*, 2002, **99**, 5804; (*c*) M. D. Curtis, J. Cao and J. W. Kampf, *J. Am. Chem. Soc.*, 2004, **126**, 4318.
7 (*a*) V. C. Sunder, J. Zaumseil, V. Podzorov, E. Menard, R. L. Willett, T. Someya, M. E. Gershenson and J. A. Rogers, *Science*, 2004, **303**, 1644; (*b*) H. Moon, R. Zeis, E.-J. Borkent, C. Besnard, A. J. Lovinger, T. Siegrist, C. Kloc and Z. Bao, *J. Am. Chem. Soc.*, 2004, **126**, 15322.
8 T. Nishinaga, N. Nodera, Y. Miyata and K. Komatsu, *J. Org. Chem.*, 2002, **67**, 6091.
9 For recent reviews, see: (*a*) J. H. Williams, *Acc. Chem. Res.*, 1993, **26**, 593; (*b*) K. Reichenbächer, H. I. Süss and J. Hulliger, *Chem. Soc. Rev.*, 2005, **34**, 22.
10 (*a*) W. Deuschel, *Helv. Chim. Acta*, 1951, **34**, 2403; (*b*) F. Ebel and W. Deuschel, *Chem. Ber.*, 1956, **89**, 2794; (*c*) D. A. Kinsley and S. G. P. Plant, *J. Chem. Soc.*, 1958, 1; (*d*) L. Chardonnens and L. Salamin, *Helv. Chim. Acta*, 1968, **51**, 1095; (*e*) L. Chardonnens, B. Laroche and W. Sieber, *Helv. Chim. Acta*, 1974, **57**, 585; (*f*) L. Chardonnens, S. Bitsch and J. Häger, *Helv. Chim. Acta*, 1975, **58**, 503; (*g*) W. Frank and R. Gompper, *Tetrahedron Lett.*, 1987, **28**, 3083; (*h*) D. Hellwinkel and T. Kistenmacher, *Liebigs Ann. Chem.*, 1989, 945; (*i*) A. Padwa, U. Chiacchio, D. J. Fairfax, J. M. Kassir, A. Litrico, M. A. Semones and S. L. Xu, *J. Org. Chem.*, 1993, **58**, 6429; (*j*) Q. Zhou, P. J. Carroll and T. M. Swager, *J. Org. Chem.*, 1994, **59**, 1294; (*k*) A. Behrendt, C. G. Screttas, D. Bethell, O. Schiemann and B. R. Steele, *J. Chem. Soc., Perkin Trans. 2*, 1998, 2039; (*l*) A. R. Helge and U. Scherf, *Synth. Met.*, 1999, **101**, 128; (*m*) S. Merlet, M. Birau and Z. Y. Wang, *Org. Lett.*, 2002, **4**, 2157.
11 J. A. R. P. Sarma and G. R. Desiraju, *Acc. Chem. Res.*, 1986, **19**, 222.
12 (*a*) A. Facchetti, Y. Deng, A. Wang, Y. Koide, H. Sirringhaus, T. J. Marks and R. H. Friend, *Angew. Chem., Int. Ed.*, 2000, **39**, 4547; (*b*) A. Facchetti, M. Mushrush, H. E. Katz and T. J. Marks, *Adv. Mater.*, 2003, **15**, 33; (*c*) A. Facchetti, M.-H. Yoon, C. L. Stern, H. E. Katz and T. J. Marks, *Angew. Chem., Int. Ed.*, 2003, **42**, 3900; (*d*) A. Facchetti, M. Mushrush, M.-H. Yoon, G. R. Hutchison, M. A. Ratner and T. J. Marks, *J. Am. Chem. Soc.*, 2004, **126**, 13859; (*e*) M.-H. Yoon, S. A. DiBenedetto, A. Facchetti and T. J. Marks, *J. Am. Chem. Soc.*, 2005, **127**, 1348; (*f*) S. Ando, J. Nishida, H. Tada, Y. Inoue, S. Tokito and Y. Yamashita, *J. Am. Chem. Soc.*, 2005, **127**, 5336.
13 (*a*) Y.-Y. Lin, D. J. Gundlach, S. F. Nelson and T. N. Jackson, *IEEE Electron Device Lett.*, 1997, **18**, 606; (*b*) S. F. Nelson, Y.-Y. Lin, D. J. Gundlach and T. N. Jackson, *Appl. Phys. Lett.*, 1998, **72**, 1854; (*c*) H. Klauk, M. Halik, U. Zschieschang, G. Schmid and W. Radlik, *J. Appl. Phys.*, 2002, **92**, 5259.
14 A. Maliakal, K. Raghavachari, H. Katz, E. Chandross and T. Siegrist, *Chem. Mater.*, 2004, **16**, 4980 and references therein.
15 For examples of short nonbonded contacts, see: (*a*) G. R. Desiraju and R. Parthasarathy, *J. Am. Chem. Soc.*, 1989, **111**, 8725; (*b*) V. R. Pedireddi, D. S. Reddy, B. S. Goud, D. C. Craig and A. D. Rae, *J. Chem. Soc., Perkin Trans. 2*, 1994, 2353; (*c*) G. R. Desiraju, *Angew. Chem., Int. Ed. Engl.*, 1995, **34**, 2311; (*d*) K. Reichenbächer, H. I. Süss and J. Hulliger, *Chem. Soc. Rev.*, 2005, **34**, 22.
16 A. Bondi, *J. Phys. Chem.*, 1964, **68**, 441.
17 (*a*) S. Hotta and K. Waragai, *J. Mater. Chem.*, 1991, **1**, 835; (*b*) G. Horowitz, B. Bachet, A. Yassar, P. Lang, F. Demanze, J.-L. Fave and F. Garnier, *Chem. Mater.*, 1995, **7**, 1337; (*c*) C. Kloc, P. G. Simpkins, T. Siegrist and R. A. Laudise, *J. Cryst. Growth*, 1997, **182**, 416; (*d*) T. Siegrist, C. Kloc, R. A. Laudise, H. E. Katz and R. C. Haddon, *Adv. Mater.*, 1998, **10**, 379; (*e*) L. Antolini, G. Horowitz, F. Kouki and F. Garnier, *Adv. Mater.*, 1998, **10**, 382; (*f*) R. Azumi, M. Goto, K. Honda and M. Matsumoto, *Bull. Chem. Soc. Jpn.*, 2003, **76**, 1561; (*g*) A.

Facchetti, M.-H. Yoon, C. L. Stern, G. R. Hutchison, M. A. Ratner and T. J. Marks, *J. Am. Chem. Soc.*, 2004, **126**, 13480.
18 The value *vs.* SCE is corrected to that *vs.* Fc/Fc^+ by addition of 0.45 V ($DMF/[NBu_4][PF_6]$). See: N. G. Connelly and W. E. Geiger, *Chem. Rev.*, 1996, **96**, 877.
19 The reduction potentials of perfluoropentacene and C_{60} were measured by differential pulse voltammograms. See: Y. Sakamoto, T. Suzuki, M. Kobayashi, Y. Gao, Y. Fukai, Y. Inoue, F. Sato and S. Tokito, *J. Am. Chem. Soc.*, 2004, **126**, 8138.
20 R. C. Haddon, A. S. Perel, R. C. Morris, T. T. M. Palstra, A. F. Hebard and R. M. Fleming, *Appl. Phys. Lett.*, 1995, **67**, 121.
21 D. J. Gundlach, J. A. Nichols, L. Zhou and T. N. Jackson, *Appl. Phys. Lett.*, 2002, **80**, 2925.
22 M. J. Frisch, G. W. Trucks, H. B. Schlegel, G. E. Scuseria, M. A. Robb, J. R. Cheeseman, V. G. Zakrzewski, J. A. Montgomery, Jr., R. E. Stratmann, J. C. Burant, S. Dapprich, J. M. Millam, A. D. Daniels, K. N. Kubin, M. C. Strain, O. Farkas, J. Tomasi, V. Barone, M. Cossi, R. Cammi, B. Mennucci, C. Pomelli, C. Adamo, S. Clifford, J. Ochterski, G. A. Petersson, P. Y. Ayala, Q. Cui, K. Morokuma, D. K. Malick, A. D. Rabuck, K. Raghavachari, J. B. Foresman, J. Cioslowski, J. V. Ortiz, B. B. Stefanov, G. Liu, A. Liashenko, P. Piskorz, I. Komaromi, R. Gomperts, R. L. Martin, D. J. Fox, T. Keith, M. A. Al-Laham, C. Y. Peng, A. Nanayakkara, C. Gonzalez, M. Challacombe, P. M. Gill, M. Head-Gordon, E. S. Replogle and J. A. Pople, *Gaussian 98, revision A.5*, Gaussian, Inc., Pittsburgh, PA, 1998.

